Bioorganic & Medicinal Chemistry Letters 23 (2013) 2313–2318

Contents lists available at SciVerse ScienceDirect

Bioorganic & Medicinal Chemistry Letters

journal homepage: www.elsevier.com/locate/bmcl

Design, synthesis and insulin-sensitising effects of novel PTP1B inhibitors

Yan-Bo Tang [a], Dianyun Lu [b], Zheng Chen [a], Chun Hu [b], Ying Yang [a], Jin-Ying Tian [c], Fei Ye [c], Li Wu [d], Zhong-Yin Zhang [d], Zhiyan Xiao [a,*]

[a] Beijing Key Laboratory of Active Substance Discovery and Druggability Evaluation, Institute of Materia Medica, Chinese Academy of Medical Sciences and Peking Union Medical College, Beijing 100050, PR China
[b] School of Pharmaceutical Engineering, Shenyang Pharmaceutical University, Shenyang 110016, PR China
[c] Beijing Key Laboratory of New Drug Mechanisms and Pharmacological Evaluation Study, Institute of Materia Medica, Chinese Academy of Medical Sciences & Peking Union Medical College, Beijing 100050, PR China
[d] Department of Biochemistry and Molecular Biology and Chemical Genomics Core Facility, Indiana University, School of Medicine, 635 Barnhill Drive, Indianapolis, IN 46202, USA

ARTICLE INFO

Article history:
Received 27 December 2012
Revised 11 February 2013
Accepted 14 February 2013
Available online 26 February 2013

Keywords:
PTP1B inhibitors
Selectivity
In vivo insulin-sensitising effects

ABSTRACT

Fifteen novel sulfathiazole-related compounds were designed as PTP1B inhibitors based on a previously reported allosteric inhibitor (**1**) of PTP1B. These compounds were synthesized and evaluated against human recombinant PTP1B. Six compounds (**3**, **4**, **8** and **14**–**16**) exhibited significant inhibitory activity against PTP1B. The most active compound (**16**) showed IC_{50} value of 3.2 μM and kinetic analysis indicated that it is a non-competitive inhibitor of PTP1B. Furthermore, compound **16** demonstrated excellent selectivity to PTP1B over other PTPs. It also displayed in vivo insulin sensitizing effect in the insulin resistant mice.

Protein tyrosine phosphatases (PTPs) play an important regulatory role in the intracellular phosphorylation state of proteins.[1] Among the PTPs, protein tyrosine phosphatase 1B (PTP1B) acts as a key negative regulator in both insulin and leptin signaling pathways, thereby modulates both glucose and lipid metabolism. The dual function of PTP1B makes it an attractive target for anti-diabetic drugs.[2,3]

Extensive medicinal chemistry efforts, especially structure-based drug design (SBDD) approaches have successfully identified a variety of potent PTP1B inhibitors (Fig. 1). However, the endeavor to develop PTP1B inhibitors into therapeutic drugs is largely unsuccessful. The attrition is due to the highly conservative and cationic nature of the PTP1B catalytic site. Most known inhibitors incorporate pTyr mimetics interacting with the catalytic site of PTP1B, thus are inherent with poor PTP1B selectivity and inadequate in vivo activity due to low cellular permeability.[3–6] Therefore, it is imperative to find novel PTP1B inhibitors acting at alternative binding sites.

An allosteric site has been described for PTP1B in 2004.[7] Small-molecule inhibitors that occupy this site block the mobility of the catalytic loop of PTP1B, so as to stabilize the inactive conformation and prevent the formation of active conformation. The allosteric site is also characterized by its non-conservative and electronically neutral constitution, which implies that targeting the allosteric site might be a feasible strategy to achieve selectivity and in vivo activity.

Benzbromarone derivative **1**, which was identified as a selective PTP1B inhibitor acting at the allosteric site, enhances insulin receptor phosphorylation in a cell-based assay and displays good selectivity over several other phosphatases.[7] These observations support the approach to overcome the selectivity and cellular permeability issues by designing and developing allosteric PTP1B inhibitors. The discovery of novel PTP1B inhibitors via pharmacophore-oriented scaffold hopping from the template structure **1** is reported herein.

The crystal structure of **1**-PTP1B complex reveals the binding mode of **1** in the allosteric site.[7] The benzofuran core is accommodated in the hydrophobic pocket formed by the side chains of the residues Leu192, Phe196 and Phe280. Two hydrogen bonds are observed between the ketone oxygen in 1 and the side chain of Asn193 as well as the sulfonamide nitrogen and the carboxyl of Glu276. An additional water-mediated hydrogen bond is detected between the phenol group and the main chain carbonyl of Phe196.

* Corresponding author. Tel.: +86 10 63189228; fax: +86 10 63017757.
E-mail address: xiaoz@imm.ac.cn (Z. Xiao).

0960-894X/$ - see front matter © 2013 Elsevier Ltd. All rights reserved.
http://dx.doi.org/10.1016/j.bmcl.2013.02.073

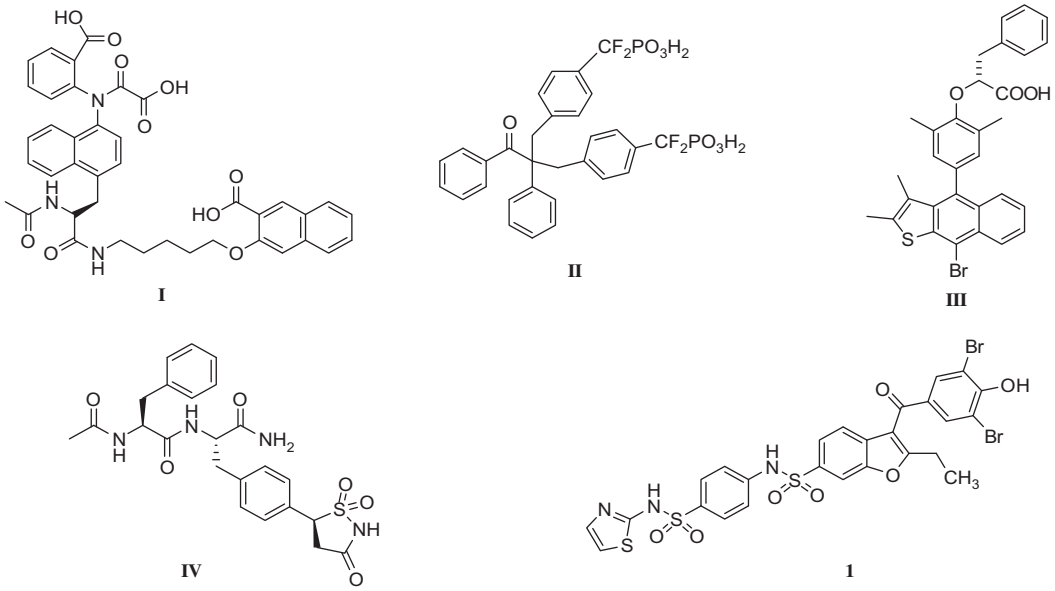

Figure 1. Structures of representative PTP1B inhibitors.

Compound **1** also adopts a 'U' shape conformation to fit the allosteric site, which allows the thiazole and the benzofuran rings to sandwich the residue Phe280 and presumably presents π–π stacking effects. Accordingly, a hypothetic pharmacophore for PTP1B allosteric inhibitors is proposed (Fig. 2).

Novel structures with the general formula illustrated in Figure 3 were designed by preserving the pharmacophric features while altering the structural skeleton of the template molecule. Virtually, the sulfathiazole part was kept intact, but the benzofuran core was replaced by substituted phenyl to improve chemical accessibility and ligand efficiency. The rest parts of the template molecule were subjected to gradual structural alteration to investigate the importance of individual pharmacophoric features. First, an amide linkage (L = –NH–) between rings A and B was maintained, and structural elements affecting the 'U' shape conformation were introduced at X, R^2 and R^3. The geometry of the sulfonamide moiety (X = $–SO_2–$, R^2 = H, R^3 = H) would allow an anti-parallel orientation of the thiazole and the phenyl (B) rings as observed in the active conformation of **1**. The amide linkage (X = –CO–, R^2 = H, R^3 = H) may also achieve a 'U' shape conformation, though is probably more energy demanding. The inclusion of salicylanilide moiety (X = –CO–, R^2 = –OH, R^3 = H) would adjust the overall conformation of the molecules via an intramolecular hydrogen bond between the amide oxygen and the *para*-hydroxyl on ring

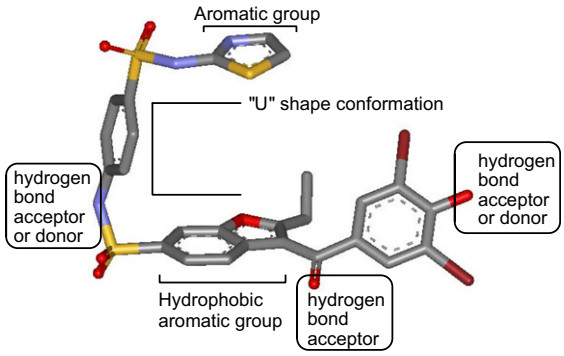

Figure 2. Hypothetic pharmacophore for PTP1B inhibitors acting at the allosteric site.

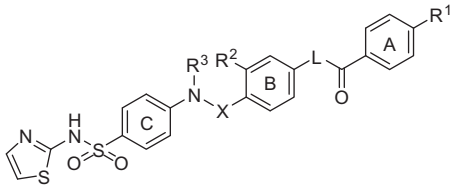

Figure 3. General formula of the target compounds.

B. While *N*-methylation of the amide bond (X = –CO–, R^2 = H, R^3 = $–CH_3–$) would also tune the general conformation of the molecules to adapt the steric hindrance posed by the methyl group. The secondary amine (X = $–CH_2–$, R^2 = H, R^3 = H) linkage with an sp^3 carbon, which would presumably be unfavorable for the 'U' shape conformation, was also introduced. After the optimal X, R^2 and R^3 were determined, the 'L' group was further elongated (L = –CH=CH– or $–CH_2–CH_2–$) to explore the possibility of forming a hydrogen bond directly between R^1 and the enzyme instead of the water-mediated interaction detected in the crystal structure of **1**-PTP1B complex. Various substituents were also introduced at R^1 to examine their effect on PTP1B inhibition.

Target molecules **2**–**12** were synthesized as shown in Schemes 1 and 2. Sulfonic acid **17** and carboxylic acids **19**, **20** were prepared from substituted benzoic acids, and were then successively reacted with oxalyl dichloride in the presence of DMF and sulfathiazole or 4-(methylamino)-*N*-(thiazol-2-yl)benzene-sulfonamide to give the target compounds **2**–**10** (Scheme 1). Reductive amination of 4-nitrobenzaldehyde with sulfathiazole was followed by reduction of the nitro group to yield **22**, which reacted with 4-methoxybenzaldehyde or 4-methoxybenzoyl chloride to provide target compounds **11** and **12**, respectively (Scheme 2).

Compounds **13**–**16** were synthesized as shown in Scheme 3. Compounds **23** were obtained via aldol condensation. Interestingly, catalytic hydrogenation of **23a** in the presence of 10% Pd/C not only saturated the double bond as expected, but also reduced the carbonyl group to hydroxyl. Such a byproduct was also ob-

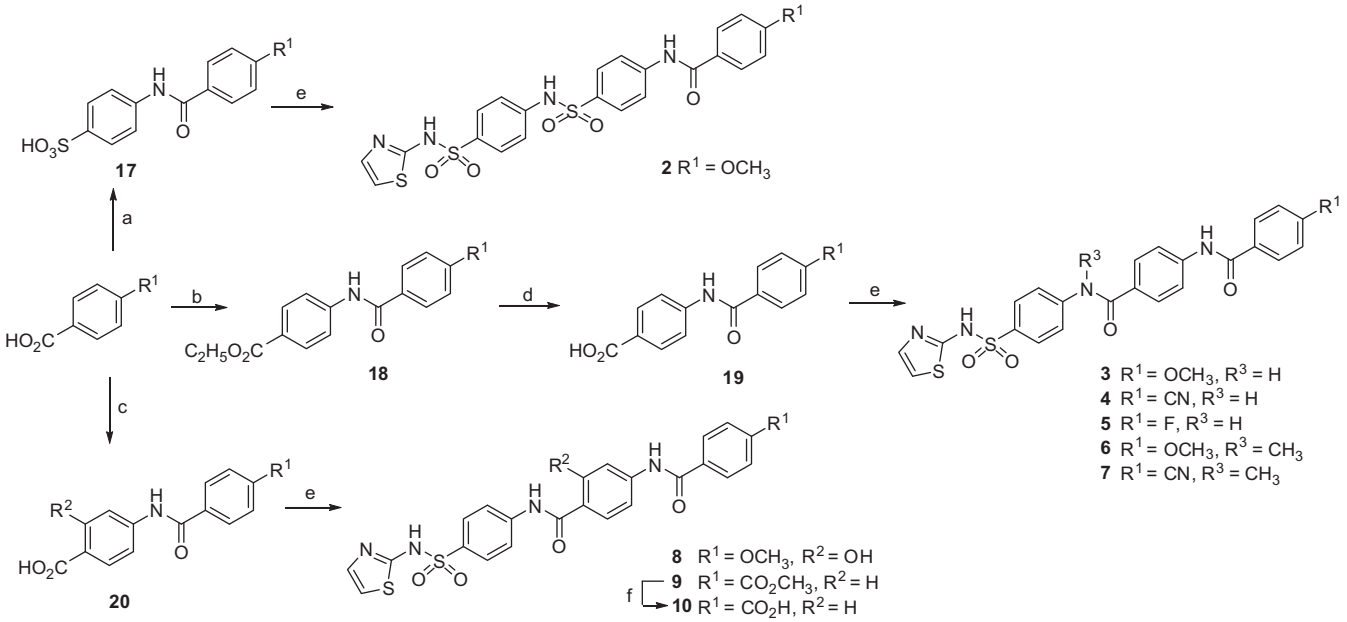

Scheme 1. Synthesis of compounds **2**–**10**. Reagents and conditions: (a) (i) $(COCl)_2$, DMF (cat), CH_2Cl_2, rt, (ii) 4-aminobenzenesulfonic acid, 0.5 M NaOH, Na_2CO_3, NBu_4Br, THF, 12 h, (iii) 1N HCl, 69%; (b) (i) $(COCl)_2$, DMF (cat), CH_2Cl_2, rt, (ii) ethyl 4-aminobenzoate, NEt_3, CH_2Cl_2, rt, 12 h, 84-87%; (c) (i) $(COCl)_2$, DMF (cat), CH_2Cl_2, rt, (ii) 4-amino benzoic acid, pyridine, THF, rt, 12 h, 44%; or 4-amino-2-hydroxybenzoic acid, acetone, rt, 12 h, 61%; (d) (i) 1 M NaOH, EtOH, 60 °C, (ii) 10% HCl, 71–88%; (e) (i) CH_2Cl_2, $(COCl)_2$, DMF (cat), rt, (ii) sulfathiazole, pyridine, acetone, rt, for **2** and **9**, 68–76%; or sulfathiazole, NEt_3, THF, rt, for **3**–**5**, 52–70%; or 4-(methylamino)-*N*-(thiazol-2-yl)benzene-sulfonamide, pyridine, acetone, rt, for **6** and **7**, 50–62%; or sulfathiazole, NEt_3, THF, rt, for **8**, 16%; (f) (i) 0.3 M NaOH, EtOH, 60 °C, (ii) 10% HCl, 50%.

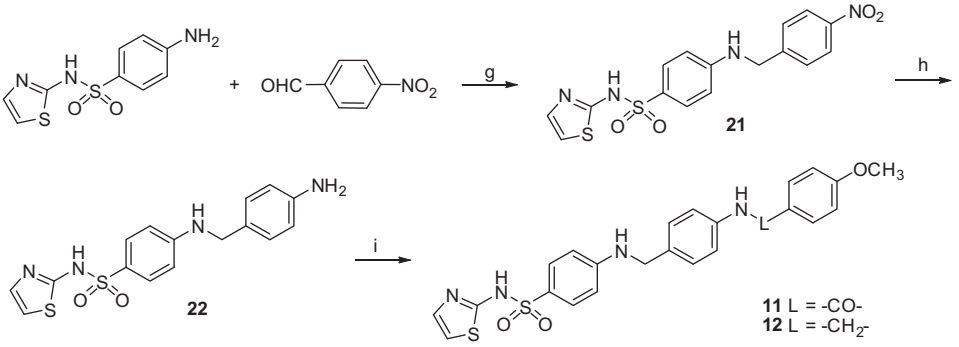

Scheme 2. Synthesis of compounds **11**–**12**. Reagents and conditions: (g) EtOH, reflux, 3 h, then $NaBH_4$, reflux, 30 min, 73%; (h) 10% Pd/C, $NaBH_4$, 2 M NaOH, H_2O, rt, 2 h, 91%; (i) 4-methoxybenzoyl chloride, NEt_3, acetone, for **11**, 30%; 4-methoxybenzaldehyde, EtOH, reflux, 2 h, then $NaBH_4$, reflux, 1 h, for **12**, 35%.

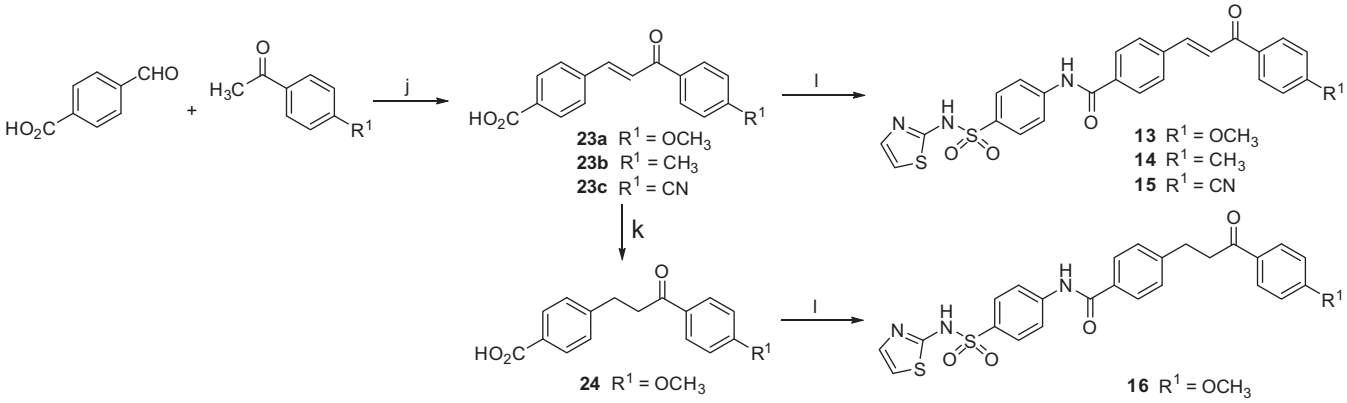

Scheme 3. Synthesis of compounds **13**–**16**. Reagents and conditions: (j) (i) NaOH, H_2O/EtOH, rt, 10 h, (ii) 20% HCl, 35–71%; (k) H_2, Pd/C, diphenyl sulfide (cat), MeOH, rt, 6 h, 96%; (l) (i) $SOCl_2$, DMF (cat), CH_2Cl_2, rt, (ii) sulfathiazole, NEt_3, CH_2Cl_2, rt, 4 h, 58–81%.

served in significant amount even with shortened reaction time. The catalyst poison diphenyl sulfide was then added to decrease the catalytic reactivity of Pd/C, and selective reduction of the double bond provided ketone **24** as the only product. The target compounds **13**–**16** were then prepared from **23** or **24** and sulfathiazole via acylation.

All target compounds were characterized by melting point, ^{1}H NMR, and mass spectra analyses.[8]

Inhibitory activity against human recombinant PTP1B: For the first round, eleven compounds (**2**–**12**) were prepared and evaluated against the human recombinant PTP1B. Most compounds showed apparent inhibition against PTP1B, and compounds **3**, **4** and **8** exhibited significant PTP1B inhibitory activity (Table 1). The results suggested preliminary structure–activities relationship (SAR) clues. Compound **2**, which had minimal structural alteration from the template structure **1**, showed moderate inhibition against PTP1B and supported the strategy of pharmacophore-oriented scaffold hopping. An amide instead of sulfonamide linkage between rings B and C improved the PTP1B inhibitory activity (**2** vs **3**). However, introducing of a methyl group at the amide nitrogen obviously decreased the activity against PTP1B (**3** vs **6**), which implies that an indispensable hydrogen bond interaction might be blocked by methylation, or alternatively, the steric hindrance at this position could impair inhibitor-enzyme interactions. The formation of intramolecular hydrogen bond exhibited no noticeable effect on PTP1B inhibition (**3** vs **8**). Furthermore, the loss of activity of compounds **11** and **12** indicated the essentiality of amide or sulfonamide linkage to ensure the active conformation. R^1 might also affect the PTP1B inhibitory activity (**3**, **4** vs **5**).

The optimal X, R^1, R^2 and R^3 were selected as X = –CO–, R^1 = –OCH_3– and R^2 = R^3 = H from the first round of synthesis. With these molecular parts fixed, the effect of the 'L' group on PTP1B inhibitory activity was further explored by replacing the amide linkage (L = –NH–) between rings A and B with vinyl or ethylene group (L = –CH=CH– or –CH_2–CH_2–), and compounds **13**–**16** were synthesized. When tested against human recombinant PTP1B, compounds **14**–**16** showed significant inhibition (Table 1), which is probably because an elongated L group brings R^1 to the vicinity of Phe196 and favors the formation of hydrogen bond interaction. Compounds **14**–**16** were further determined for their IC_{50} values against PTP1B (Table 2). All of them showed IC_{50} values comparable or even superior to that of **1**.

To determine whether compound **16** inhibits PTP1B in a non-competitive manner, its effect on PTP1B-catalyzed *p*NPP hydrolysis was examined.[10] As evidenced by the Lineweaver-Burk plot (Fig. 4), compound **16** is indeed a non-competitive inhibitor with a K_i value of 5.8 ± 0.3 μM.

*Selectivity of compounds **14**–**16** against a panel of PTPs*: Compounds **14**–**16** were evaluated against a panel of PTPs, including PTP1B, SHP2 (Src homology2 domain containing phosphotyrosine phosphatase 2), VHR (human vaccinia H1-related phosphatase), LYP (lymphoid-specific protein tyrosine phosphatase), PTPα (protein tyrosine phosphatase α), TC-PTP (T-cell protein tyrosine phosphatase) and CDC25 (cell division cycle 25 phosphatases).[10] The IC_{50} values of compounds **14**–**16** against the seven PTPs were reported in Table 3. Impressively, compound **16** showed significant selectivity to PTP1B over TC-PTP, the most homologous enzyme of PTP1B in the PTPs family.

A docking study[11] of compound **16** indicated that it interacted with the allosteric site of PTP1B in a way similar to that of the template structure **1**. The phenyl B ring situates in the hydrophobic pocket formed by the side chains of Ala189, Leu192 and Phe280. π–π stacking interaction was observed between the thiazole ring and Phe280. Hydrogen bond interactions are also monitored between the ketone oxygen in **16** and Asn193 as well as the amide nitrogen and Glu276 (Fig. 5).

In vivo insulin-sensitising effects: Compound **16** was further examined for its in vivo insulin-sensitising effects with the hyperinsulinemic–euglycemic clamp test.[9] Insulin resistant model (IRM) obesity mice were induced by high-fat diet (HFD) as previously described.[9] The insulin sensitizer Rosiglitazone was used as a positive control. As illustrated in Fig. 6, the glucose infusion rate (GIR) values in the IRM model mice were decreased significantly as compared with those of mice in the blank control group (Con) (12.8 ± 2.8 vs 2.1 ± 0.2 mg/min/kg), which indicated the validity of the HFD-induced insulin resistance model. While oral administration of Rosiglitazone (Rosi) and compound **16** to IR mice in-

Table 1
Percentage inhibition of the tested compounds against human recombinant PTP1B[9]

Compd	Percentage inhibition[a] (%)	Compd	Percentage inhibition[a] (%)	Compd	Percentage inhibition[a] (%)
2	45.3	7	23.8	12	NA
3	81.9	8	78.1	13[b]	20.7
4	87.1	9	NA	14[b]	79.8
5	53.1	10	NA	15[b]	68.9
6	24.6	11	NA	16[b]	75.7

NA: Not active, no noticeable inhibition was observed under the test concentration.
[a] The percentage inhibition was measured under the concentration of 100 μM, except other specified.
[b] The percentage inhibition was measured under the concentration of 10 μM.

Table 2
PTP1B inhibitory activity of compounds **14**–**16**[10]

Compd	**14**	**15**	**16**	**1**[a]
IC_{50} (μM)	8.3 ± 0.3	8.1 ± 0.3	3.2 ± 0.1	8

[a] The IC_{50} value of compound **1** was taken from Ref. 7.

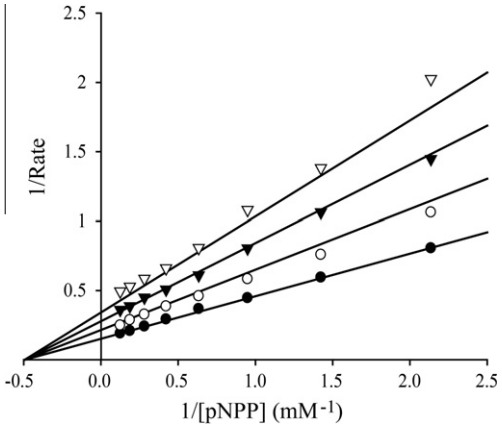

Figure 4. Kinetic analysis of the inhibition against PTP1B-catalyzed *p*NPP hydrolysis by compound **16**. The tested concentrations were 0 (●), 2.5 (○), 5 (▲), and 7.5 (Δ) μM, respectively.

Table 3
Selective inhibitory activity against PTPs[10]

IC_{50} (M)	**14**	**15**	**16**
PTP1B	8.3 ± 0.3	8.1 ± 0.3	3.2 ± 0.1
SHP2	6.9 ± 0.6	7.8 ± 0.8	8.0 ± 1.0
VHR	9.0 ± 0.9	9.2 ± 0.7	>10
LYP	10.4 ± 0.3	8.0 ± 0.4	>10
PTP	ND[a]	ND	>10
TC-PTP	ND	ND	40 ± 10
CDC25	ND	ND	>100

[a] ND: not determined.

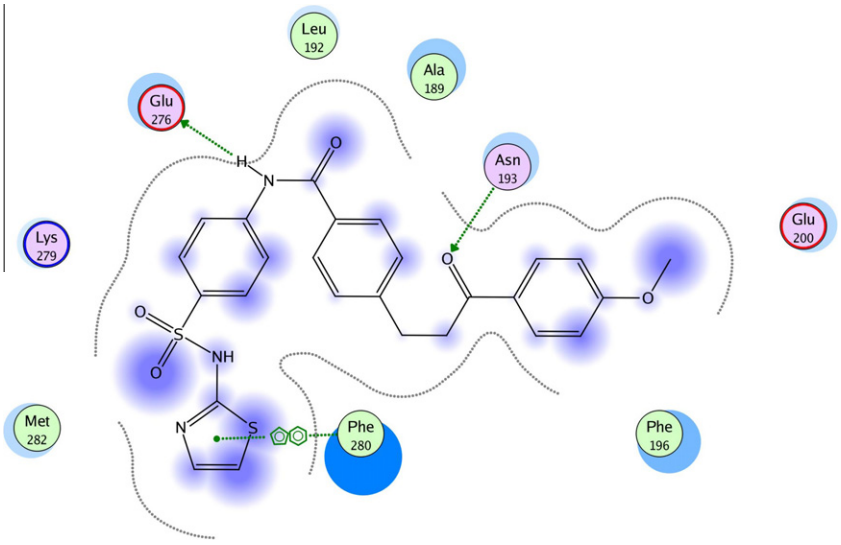

Figure 5. Interaction mode of compound **16** with the allosteric site of PTP1B.

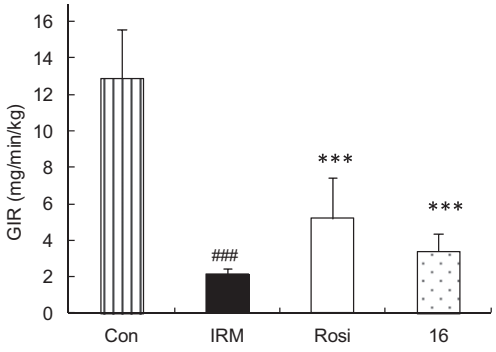

Figure 6. Glucose infusion rates (GIR) in hyperinsulinemic–euglycemic clamp test ($n = 8$).[9] $^{###}P$ <0.001 versus Con; $^{***}p$ <0.001 versus IRM.

creased the GIR values to 243% and 148%, respectively. These observations implicated that similar to Rosiglitazone, compound **16** could ameliorated the impaired insulin sensitivity in IRM mice.

In conclusion, a series of novel PTP1B inhibitors were designed based on the template structure **1**. Biological evaluation identified compound **16** as a new and non-competitive PTP1B inhibitor. Excellent selectivity over a panel of PTPs and significant in vivo insulin sensitizing effect were achieved. The current results support the strategy to target the allosteric binding site of PTP1B as an approach to overcome the poor selectivity and inadequate in vivo activity associated with most of the known potent PTP1B inhibitors. Further hit evolution following this molecular design are undergoing and will be reported in due course.

Acknowledgments

This research work was financially supported by National Natural Science Foundation of China (20972192) and Beijing Natural Science Foundation (7102117) awarded to Z.X., National S & T Major Project (2012ZX09103-101-063) to F.Y. and National Institutes of Health Grant (CA152194) to Z.-Y.Z.

Supplementary data

Supplementary data (supplementary information on general preparation procedures is available online. Biological assays were performed by following experimental protocols in the cited references without modification) associated with this article can be found, in the online version, at http://dx.doi.org/10.1016/j.bmcl.2013.02.073.

References and notes

1. Barr, A. J. *Future Med. Chem.* **2010**, *2*, 1563.
2. Montalibet, J.; Kennedy, B. P. *Drug Discovery Today Ther. Strateg.* **2005**, *2*, 129.
3. Zhang, S.; Zhang, Z. *Drug Discovery Today* **2007**, *12*, 373.
4. Combs, A. P. *J. Med. Chem.* **2010**, *53*, 2333.
5. Lee, S.; Wang, Q. *Med. Res. Rev.* **2007**, *27*, 553.
6. Nichols, A. J.; Mashal, R. D.; Balkan, B. *Drug Dev. Res.* **2006**, *67*, 559.
7. Wiesmann, C.; Barr, K. J.; Kung, J.; Zhu, J.; Erlanson, D. A.; Shen, W.; Fahr, B. J.; Zhong, M.; Taylor, L.; Randal, M.; McDowell, R. S.; Hansen, S. K. *Nat. Struct. Mol. Biol.* **2004**, *11*, 730.
8. *Compound* ***2***: Yield 68%; whitish solid; mp 239–241 °C; ^{1}H NMR (300 MHz, DMSO-d_6): δ 3.84 (s, 3H), 6.80 (d, 1H, J = 4.2 Hz), 7.07 (d, 2H, J = 8.1 Hz), 7.18–7.25 (m, 3H), 7.66 (d, 2H, J = 8.1 Hz), 7.79 (d, 2H, J = 8.7 Hz), 7.94 (m, 4H), 10.44 (s, 1H), 10.75 (s, 1H), 12.67 (s, 1H); FAB-MS: m/z 545 [M+H]$^+$. *Compound* ***3***: Yield 59%; whitish solid; mp >350 °C; ^{1}H NMR (300 MHz, DMSO-d_6): δ 3.85(s, 3H), 6.82 (d, 1H, J = 3.9 Hz), 7.09 (t, 2H, J = 8.7 Hz), 7.26 (d, 1H, J = 3.9 Hz), 7.79 (d, 2H, J = 8.7 Hz), 7.93–8.01 (m, 8H), 10.38(s, 1H), 10.46 (s, 1H), 12.71 (s, 1H); FAB-MS: m/z 509 [M+H]$^+$. *Compound* ***4***: Yield 52%; light yellow solid; mp 301–304 °C; ^{1}H NMR (300 MHz, DMSO-d_6): δ 6.83 (d, 1H, J = 4.5 Hz), 7.26 (d, 1H, J = 4.5 Hz), 7.79 (d, 2H, J = 8.7 Hz), 7.93–8.07 (m, 8H), 8.14 (d, 2H, J = 8.4 Hz), 10.48 (s, 1H), 10.76 (s, 1H), 12.71 (s, 1H); FAB-MS: m/z 504 [M+H]$^+$. *Compound* ***5***: Yield 70%; whitish solid; mp 307–309 °C; ^{1}H NMR (300 MHz, DMSO-d_6): δ 6.83 (d, 1H, J = 4.5 Hz), 7.26 (d, 1H, J = 4.5 Hz), 7.40 (t, 2H, J = 9.0 Hz), 7.79 (d, 2H, J = 9.0 Hz), 7.93–8.10 (m, 8H), 10.47 (s, 1H), 10.55 (s, 1H), 12.70 (s, 1H); FAB-MS: m/z 497 [M+H]$^+$. *Compound* ***6***: Yield 62%; whitish solid; mp 208–212 °C; ^{1}H NMR (300 MHz, DMSO-d_6): δ 3.39 (s, 3H), 3.83 (s, 3H), 6.83 (d, 1H, J = 4.5 Hz), 7.05 (d, 2H, J = 8.4 Hz), 7.24–7.32 (m, 5H), 7.65 (d, 2H, J = 7.8 Hz), 7.68 (d, 2H, J = 8.7 Hz), 7.93 (d, 2H, J = 8.4 Hz), 10.17 (s, 1H), 12.76 (s, 1H); EI-MS: m/z 522 [M]$^+$. *Compound* ***7***: Yield 50%; whitish solid; mp 248–251 °C; ^{1}H NMR (300 MHz, DMSO-d_6): δ 3.39 (s, 3H), 6.83 (d, 1H, J = 4.5 Hz), 7.25 (d, 1H, J = 4.5 Hz), 7.28 (d, 2H, J = 8.4 Hz), 7.31 (d, 2H, J = 8.4 Hz), 7.64 (d, 2H, J = 8.4 Hz), 7.67 (d, 2H, J = 8.4 Hz), 8.02 (d, 2H, J = 8.1 Hz), 8.07 (d, 2H, J = 8.1 Hz), 10.56 (s, 1H), 12.75 (s, 1H); FAB-MS: m/z 518 [M+H]$^+$. *Compound* ***8***: Yield 16%; whitish solid; mp 309–311 °C; ^{1}H NMR (300 MHz, DMSO-d_6): δ 3.84 (s, 3H), 6.82 (d, 1H, J = 4.5 Hz), 7.08 (d, 2H, J = 7.8 Hz), 7.24 (d, 1H,, J = 4.5 Hz), 7.34 (d, 1H, J = 8.7 Hz), 7.65 (s, 1H), 7.78 (d, 2H, J = 7.8 Hz), 7.86 (d, 2H, J = 7.8 Hz), 7.90–8.05 (m, 3H), 10.28 (s, 1H), 10.51 (s, 1H), 11.88 (s, 1H), 12.70 (s, 1H); FAB-MS: m/z 525 [M+H]$^+$. *Compound* ***9***: Yield 76%; whitish solid; mp >350 °C; ^{1}H NMR (300 MHz, DMSO-d_6): δ 3.91 (s, 3H), 6.66 (d, 1H, J = 4.5 Hz), 7.12 (d, 1H, J = 4.5 Hz), 7.76 (d, 2H, J = 8.7 Hz), 7.89 (d, 2H, J = 8.7 Hz), 7.96 (d, 2H, J = 8.7 Hz), 8.01 (d, 2H, J = 8.7 Hz), 8.12 (s, 4H), 10.43 (s, 1H), 10.75 (s, 1H); ESI-MS: m/z 537 [M+H]$^+$. *Compound* ***10***: Yield 50%; whitish solid; mp >350 °C; ^{1}H NMR (300 MHz, DMSO-d_6): δ 6.68 (d, 1H, J = 4.2 Hz), 7.14 (d, 1H, J = 4.2 Hz), 7.75 (d, 2H, J = 8.7 Hz), 7.89 (d, 2H, J = 8.7 Hz), 7.94–8.05 (m, 8H), 10.44 (s, 1H), 10.67 (s, 1H); ESI-MS: m/z 523 [M+H]$^+$. *Compound* ***11***: Yield 50%; whitish solid; mp 233–236 °C; ^{1}H NMR (300 MHz, DMSO-d_6): δ 3.84 (s, 3H), 4.27 (d, 2H, J = 5.4 Hz), 6.61 (d, 2H, J = 8.7 Hz), 6.74 (d, 1H, J = 4.5 Hz), 6.99 (t, 1H, J = 5.4 Hz), 7.05 (d, 2H, J = 8.7 Hz), 7.18 (d, 1H, J = 4.5 Hz), 7.29 (d, 2H, J = 8.7 Hz), 7.47 (d, 2H, J = 8.7 Hz), 7.70 (d,

2H, J = 8.7 Hz), 7.95 (d, 2H, J = 8.7 Hz), 10.06 (s, 1H), 12.42 (s, 1H); ESI-MS: m/z 495 $[M+H]^+$. *Compound* ***12***: Yield 35%; mp 111–113 °C; ^{1}H NMR (300 MHz, DMSO-d_6): δ 3.71 (s, 3H), 4.07 (d, 2H, J = 6.0 Hz), 4.15 (d, 2H, J = 6.0 Hz), 6.09 (t, 1H, J = 6.0 Hz), 6.52 (d, 2H, J = 8.7 Hz), 6.58 (d, 2H, J = 8.7 Hz), 6.73 (d, 1H, J = 4.5 Hz), 6.76 (t, 1H, J = 6.0 Hz), 6.86 (d, 2H, J = 8.7 Hz), 7.00 (d, 2H, J = 8.7 Hz), 7.18 (d, 1H, J = 4.5 Hz), 7.25 (d, 2H, J = 8.7 Hz), 7.44 (d, 2H, J = 8.7 Hz), 12.42 (s, 1H); ESI-MS: m/z 481 $[M+H]^+$. *Compound* ***13***: Yield 58%; light yellow solid; mp 235–237 °C; ^{1}H NMR (300 MHz, DMSO-d_6): δ 3.87 (s, 3H), 6.82 (d, 1H, J = 4.5 Hz), 7.10 (d, 2H, J = 8.7 Hz), 7.25 (d, 1H, J = 4.5 Hz), 7.73–7.81 (m, 3H), 7.94 (d, 2H, J = 8.7 Hz), 7.99–8.10 (m, 5H), 8.19 (d, 2H, J = 8.7 Hz), 10.62 (s, 1H), 12.70 (s, 1H); HR-ESI-MS: m/z 520.0983 $[M+H]^+$ (calcd for $C_{26}H_{22}N_3O_5S_2$: 520.1001). *Compound* ***14***: Yield 74%; light yellow solid; mp 220–223 °C; ^{1}H NMR (300 MHz, DMSO-d_6): δ 2.41 (s, 3H), 6.82 (d, 1H, J = 4.5 Hz), 7.25 (d, 1H, J = 4.5 Hz), 7.39 (d, 2H, J = 7.8 Hz), 7.75–7.81 (m, 3H), 7.94 (d, 2H, J = 8.7 Hz), 7.99–8.11 (m, 7H), 10.62 (s, 1H), 12.70 (s, 1H); HR-ESI-MS: m/z 504.1027 $[M+H]^+$ (calcd for $C_{26}H_{22}N_3O_4S_2$: 504.1052). *Compound* ***15***: Yield 78%; light yellow solid; mp 260–262 °C; ^{1}H NMR (300 MHz, DMSO-d_6): δ 6.81 (d, 1H, J = 4.5 Hz), 7.24 (d, 1H, J = 4.5 Hz), 7.77–7.86 (m, 4H), 7.94 (d, 2H, J = 8.4 Hz), 8.01–8.09 (m, 6H), 8.31 (d, 2H, J = 8.7 Hz), 10.62 (s, 1H), 12.62 (br, 1H); HR-ESI-MS: m/z 515.0836 $[M+H]^+$ (calcd for $C_{26}H_{19}N_4O_4S_2$: 515.0848). *Compund* ***16***: Yield 81%; whitish solid; mp 245–247 °C; ^{1}H NMR (300 MHz, DMSO-d_6): δ 3.00 (t, 2H, J = 7.2 Hz), 3.37 (t, 2H, J = 7.2 Hz), 3.82 (s, 3H), 6.81 (d, 1H, J = 4.5 Hz), 7.02 (d, 2H, J = 8.7 Hz), 7.24 (d, 1H, J = 4.5 Hz), 7.44 (d, 2H, J = 8.1 Hz), 7.76 (d, 2H, J = 9.0 Hz), 7.85–7.98 (m, 6H), 10.45 (s, 1H), 12.69 (s, 1H); HR-ESI-MS: m/z 522.1135 $[M+H]^+$ (calcd for $C_{26}H_{24}N_3O_5S_2$: 522.1157).

9. The measurements were performed by following the experimental protocols described in this cited reference Ma, Y.-M.; Tao, R.-Y.; Liu, Q.; Li, J.; Tian, J.-Y.; Zhang, X.-L.; Xiao, Z.-Y.; Ye, F. *Mol. Cell. Biochem.* **2011**, *357*, 65.
10. The measurements were performed by following the experimental protocols described in the cited references (a) Liu, S.; Zeng, L.-F.; Wu, L.; Yu, X.; Xue, T.; Gunawan, A. M.; Long, Y.-Q.; Zhang, Z.-Y. *J. Am. Chem. Soc.* **2008**, *130*, 17075; (b) He, R.; Zeng, L.-F.; He, Y.; Zhang, S.; Zhang, Z.-Y. *FEBS J.* **2013**, *280*, 731.
11. The structure of compound **16** was generated and molecular docking was performed with the Discovery Studio 2.5 software package (Accelrys, San Diego, USA).The complex structure of **1**-PTP1B was obtained from the Protein Data Bank (PDB code: 1t4j). The docking calculation was carried out with the LibDock protocol. Default settings were used. All calculations were performed on a DELL Precision T5500 workstation. The Ligand Interactions tool in MOE (Chemical Computing Group, Inc., Montreal, Quebec, Canada) was used to plot the 2D interaction modes.